

Please cite this article in press as: Carey LM et al. Small molecule inhibitors of PSD95–nNOS protein–protein interactions suppress formalin-evoked Fos protein expression and nociceptive behavior in rats. *Neuroscience* (2017), <http://dx.doi.org/10.1016/j.neuroscience.2017.02.055>

Neuroscience xxx (2017) xxx–xxx

SMALL MOLECULE INHIBITORS OF PSD95–nNOS PROTEIN–PROTEIN INTERACTIONS SUPPRESS FORMALIN-EVOKED Fos PROTEIN EXPRESSION AND NOCICEPTIVE BEHAVIOR IN RATS

LAWRENCE M. CAREY,^{a,b} WAN-HUNG LEE,^c
TANNIA GUTIERREZ,^a PUSHKAR M. KULKARNI,^d
GANESH A. THAKUR,^d YVONNE Y. LAI^{a,e} AND
ANDREA G. HOHMANN^{a,b,c,f,*}

^a Department of Psychological and Brain Sciences, Indiana University, Bloomington, IN, United States

^b Program in Neuroscience, Indiana University, Bloomington, IN, United States

^c Interdisciplinary Biochemistry Program, Molecular and Cellular Biochemistry Department, Indiana University, Bloomington, IN, United States

^d Center for Drug Discovery, and Department of Pharmaceutical Sciences, Northeastern University, Boston, MA, United States

^e Anagin, Inc., Indianapolis, IN, United States

^f Gill Center for Biomolecular Science, Indiana University, Bloomington, IN, United States

decreased the number of formalin-induced Fos-like immunoreactive cells in spinal dorsal horn regions associated with nociceptive processing. MK-801 suppressed Fos protein expression in both dorsal and ventral horns. MK-801 produced motor ataxia in the rotarod test whereas IC87201 and ZL006 failed to do so. ZL006 but not ZL007 suppressed paclitaxel-induced mechanical and cold allodynia in a model of chemotherapy-induced neuropathic pain. Co-immunoprecipitation experiments revealed the presence of the PSD95–nNOS complex in lumbar spinal cord of paclitaxel-treated rats, although ZL006 did not reliably disrupt the complex in all subjects. The present findings validate use of putative small molecule PSD95–nNOS protein–protein interaction inhibitors as novel analgesics and demonstrate, for the first time, that these inhibitors suppress inflammation-evoked neuronal activation at the level of the spinal dorsal horn. © 2017 Published by Elsevier Ltd on behalf of IBRO.

Abstract—Excessive activation of NMDA receptor (NMDAR) signaling within the spinal dorsal horn contributes to central sensitization and the induction and maintenance of pathological pain states. However, direct antagonism of NMDARs produces undesirable side effects which limit their clinical use. NMDAR activation produces central sensitization, in part, by initiating a signaling cascade that activates the enzyme neuronal nitric oxide synthase (nNOS) and generates the signaling molecule nitric oxide. NMDAR-mediated activation of nNOS requires a scaffolding protein, postsynaptic density protein 95 kDa (PSD95), which tethers nNOS to NMDARs. Thus, disrupting the protein–protein interaction between PSD95 and nNOS may inhibit pro-nociceptive signaling mechanisms downstream of NMDARs and suppress central sensitization while sparing unwanted side effects associated with NMDAR antagonists. We examined the impact of small molecule PSD95–nNOS protein–protein interaction inhibitors (ZL006, IC87201) on both nociceptive behavior and formalin-evoked Fos protein expression within lumbar spinal dorsal horn of rats. Comparisons were made with ZL007, an inactive analog of ZL006, and the NMDAR antagonist MK-801. IC87201 and ZL006, but not ZL007, suppressed phase 2 of formalin-evoked pain behavior and

Key words: *N*-methyl-D-aspartate receptor, neuronal nitric oxide synthase, postsynaptic density protein 95 kDa, protein–protein interaction inhibitor, central sensitization, dorsal horn.

INTRODUCTION

Intense activation of peripheral nociceptors can drive neuroplastic alterations in neuronal circuitry within the central nervous system (CNS) leading to increased excitability and synaptic efficacy, a phenomenon known as central sensitization (Ji and Woolf, 2001). Sensitization of CNS neuronal circuitry can produce exaggerated responses to both noxious and non-noxious stimulation, resulting in hyperalgesia and allodynia, respectively. The increased reactivity of spinal neuronal circuitry initiated by central sensitization may contribute to the development of a wide range of pathological pain states including neuropathic and inflammatory pain conditions (see Latremoliere and Woolf, 2009 for review). Glutamatergic signaling through the *N*-methyl-D-aspartate receptor (NMDAR) is an important mechanism involved in the generation of central sensitization (Woolf and Thompson, 1991; Ma and Woolf, 1995; South et al., 2003). NMDAR antagonists produce antinociceptive efficacy in various animal models of pain (see Zhou et al., 2011 for review). However, the clinical use of direct NMDAR antagonists is problematic as they produce deleterious side effects including learning and memory deficits, cognitive

*Correspondence to: A. G. Hohmann, Department of Psychological & Brain Sciences, Indiana University, 1101 East 10th street, Bloomington, IN 47405-7007, USA. Fax: +1-813-856-7187.

E-mail address: hohmanna@indiana.edu (A. G. Hohmann).

Abbreviations: AUC, area under the curve; CNS, central nervous system; CPS, composite pain scores; eNOS, endothelial nitric oxide synthase; FLI, Fos-like immunoreactive; i.p., intraperitoneal; NMDAR, *N*-methyl-D-aspartate receptor; nNOS, neuronal nitric oxide synthase; NO, nitric oxide; PSD95, postsynaptic density 95 kDa.

dysfunction, motor impairment, dissociation from reality and abuse liability (Krystal et al., 1994; Pal et al., 2002).

Activation of NMDARs leads to calcium influx in the postsynaptic cell, an event that activates signaling pathways involved in the induction of plasticity implicated in pathological pain states (Ji et al., 2003). Following entry via NMDARs, calcium binds to calmodulin, which in turn activates the enzyme neuronal nitric oxide synthase (nNOS), which generates the signaling molecule nitric oxide (NO). Excess NO production is involved in pain signaling and the development of central sensitization (Kitto et al., 1992; Aley et al., 1998; Wu et al., 2001; Miclescu and Gordh, 2009). NMDAR-mediated production of NO relies on the tethering of nNOS to NMDARs via the scaffolding protein postsynaptic density 95 kDa (PSD95). Thus, decreasing PSD95 expression with antisense oligonucleotides attenuates NMDAR-mediated production of NO and cell death (Sattler et al., 1999) and knockdown of PSD95 expression within the spinal cord also decreases NMDA-induced thermal hyperalgesia (Tao et al., 2000), and delays the onset of mechanical and thermal hyperalgesia induced by spinal nerve ligation (Tao et al., 2001). These observations collectively suggest that the NMDAR–PSD95–nNOS complex may play a key role in the development of central sensitization.

Small molecules capable of disrupting PSD95–nNOS protein–protein interactions have recently been developed and show efficacy in preclinical models assessing pain behavior (Florio et al., 2009; Lee et al., 2015), depression-like behavior (Doucet et al., 2013), and neuroprotection following cerebral ischemia (Zhou et al., 2010). IC87201, a first in class PSD95–nNOS inhibitor, displays antinociceptive efficacy in rodent models of inflammatory and neuropathic pain when administered intrathecally (Florio et al., 2009) or when administered systemically in mice (Lee et al., 2015). Our recent studies showed that IC87201 and ZL006, a related molecule, disrupt binding of PSD95 and nNOS *in vitro*, suppress glutamate-induced excitotoxicity and attenuate inflammatory and neuropathic pain behavior in mice (Lee et al., 2015). Furthermore, IC87201 and ZL006 did not alter basal nociceptive thresholds in the absence of pain or produce motor ataxia (Lee et al., 2015) or memory impairments characteristic of the non-competitive NMDAR antagonist MK-801 (Smith et al., 2016). Thus, disruption of PSD95–nNOS protein–protein interactions may represent a novel, therapeutic mechanism for managing pathological pain that lacks problematic side effects associated with direct NMDAR antagonists. However, *in vivo* studies relying on assessments of pain behavior are not sufficient to conclude that PSD95–nNOS inhibitors act at a neural level to suppress the processing of nociceptive information. This conclusion requires the demonstration that PSD95–nNOS inhibitors disrupt the processing of nociceptive information.

Whether IC87201 and ZL006 suppress nociceptive processing and CNS sensitization associated with pathological pain is unknown. ZL006, but not a related analog, ZL007, disrupts co-immunoprecipitation of nNOS and PSD95 in hippocampal slice cultures (Zhou et al., 2010), suggesting that ZL007 may be a useful

inactive analog to confirm mechanism of action of active PSD95–nNOS inhibitors. However, to our knowledge, the *in vivo* profile of this compound has never been characterized and whether or not ZL006 shows antinociceptive efficacy in rats is unknown. We, therefore, used IC87201, ZL006 and the putative inactive analog ZL007, to ask whether small molecule inhibitors of PSD95–nNOS protein–protein interactions alter neurochemical markers of inflammation-evoked neuronal activity at the level of the lumbar spinal dorsal horn in rats. Importantly, we evaluated whether systemically administered IC87201 and ZL006 decrease formalin-evoked nociceptive behavior and formalin-evoked Fos-like immunoreactivity in the lumbar spinal dorsal horn within the same subjects. We also evaluated whether IC87201 and ZL006, administered systemically, produce motor ataxia in rats using the rotarod test. Comparisons were made with the non-competitive NMDAR antagonist MK-801 and the putative inactive analog ZL007. Next we used ZL006, which has previously been shown to disrupt interactions between PSD95 and nNOS (but not NMDAR subunit NR2B-PSD95 (Zhou et al., 2010) or ERB4-PSD95 interactions (Lee et al., 2015) and maximally reduced formalin-evoked nociceptive behavior and dorsal horn Fos protein expression in our studies, to test the hypothesis that ZL006 but not ZL007 would reduce paclitaxel-induced neuropathic pain in rats. Finally, using co-immunoprecipitation, we evaluated whether paclitaxel-induced neuropathic pain promotes the formation of the PSD95–nNOS complex in the spinal cord *in vivo*, and whether systemic treatment with ZL006 could prevent the association of nNOS and PSD95 in lumbar spinal cord tissue. The results of our study demonstrate, for the first time, that ZL006 produces antinociception in rats whereas ZL007 is ineffective. We also show that IC87201 produces antinociception in rats following systemic administration. Finally, our studies show that the PSD95–nNOS complex is present in the lumbar spinal cord and also show that PSD95–nNOS protein–protein interaction inhibitors concomitantly suppress noxious stimulus-evoked increases in neuronal activation within spinal cord regions implicated in nociceptive processing as well as pain behavior in a manner that is selective for active but not inactive analogs.

EXPERIMENTAL PROCEDURES

Subjects

One hundred and eleven male Sprague–Dawley rats (285–446 g; Envigo, Indianapolis, IN, USA) were used in these experiments. All procedures were approved by the Bloomington Institutional Animal Care and Use Committee (BIACUC) of Indiana University. Animals were housed in a temperature-controlled facility with free access to food and water in their home cages on a regular 12-h light/dark cycle.

Drugs and chemicals

ZL006, IC87201 and ZL007 were synthesized in the laboratory of Dr. Ganesh Thakur (by P.M.K.) at the

165 Northeastern University Center for Drug Discovery
166 (Boston, MA, USA). MK-801 and formaldehyde (37% in
167 H₂O) were purchased from Sigma Aldrich (St. Louis,
168 MO, USA). All drugs were dissolved in a vehicle of 20%
169 dimethyl sulfoxide (Sigma Aldrich, St. Louis, MO, USA),
170 with the remaining 80% consisting of 95% ethanol
171 (Sigma Aldrich, St. Louis, MO, USA), emulphor
172 (Alkamuls EL 620L; Solvay) and 0.9% saline (Aquilite
173 System; Hospira, Inc, Lake Forest, IL, USA) at a ratio of
174 1:1:8, respectively for intraperitoneal (i.p.) administration
175 and administered at a volume of 1 ml/kg. Formalin was
176 diluted from formaldehyde stock (100% formalin) in
177 sterile saline to a final concentration of 2.5% and
178 administered in a volume of 50 μ l. Paclitaxel was
179 purchased from Tecoland (Irvine, CA, USA) and was
180 dissolved in a vehicle consisting of cremophor EL
181 (Sigma–Aldrich, St. Louis, MO, USA), 95% ethanol
182 (Sigma Aldrich, St. Louis, MO, USA) and saline at a
183 ratio of 1:1:18 respectively and was administered at a
184 volume of 1 ml/kg.

185 Formalin test

186 Rats received a single i.p. injection of ZL006 (4 or 10 mg/
187 kg) ZL007 (10 mg/kg), IC87201 (4 or 10 mg/kg), MK-801
188 (0.1 mg/kg) or vehicle 30 min prior to intraplantar (i.pl.)
189 injection of formalin. Animals were placed in an
190 elevated, clear Plexiglas observation chamber
191 immediately after i.p. injection and allowed to habituate
192 to the observation chamber for 30 min. Following
193 habituation, rats received a unilateral intradermal
194 injection (50 μ l) of 2.5% formalin into the superficial
195 plantar surface of the hind paw. Nociceptive behaviors
196 were video recorded over 60 min immediately following
197 formalin injection and quantified from videotapes by a
198 single rater (LMC) who was blinded to the experimental
199 conditions. Composite pain scores (CPS) were
200 calculated for every 5 min bin for the total duration of
201 60 min using the following scoring criteria: no behavior
202 was scored 0, lifting was scored 1, and shaking/biting/
203 flinching was scored as 2. The area under the curve
204 (AUC) of pain behavior was calculated for both the early
205 (phase 1, 0–10 min) and the late (phase 2, 10–60 min)
206 for each subject as described in our previous work
207 (Guindon et al., 2011).

208 Rotarod test

209 Motor performance was assessed in separate groups of
210 rats using an accelerating Rotarod (IITC Life Science)
211 (4–40 rpm, 300 s cutoff time) as performed in our
212 previous work (Rahn et al., 2011). Rats were trained over
213 two consecutive days and on the third day baseline laten-
214 cies to descend from the rotating drum were measured.
215 Following acquisition of baseline measurements, rats
216 received a single i.p. injection of ZL006 (10 mg/kg),
217 IC87201 (10 mg/kg), MK-801 (0.1 mg/kg) or vehicle. At
218 30 and 60 min following i.p. injection, rats were placed
219 on the accelerating rotarod and the descent latency was
220 recorded in duplicate. Animals that did not meet exclusion
221 criteria (i.e. ability to stay on rotating drum for at least 30 s
222 on baseline day) were removed from the study and did not

receive any pharmacological treatments. The experi- 223
menter was always blinded to the experimental conditions. 224

Tissue preparation for immunohistochemistry 225

226 Immunohistochemical procedures were carried out in
227 the same subjects used to assess antinociception in the
228 formalin test. Immediately following conclusion of
229 the formalin behavioral assay (i.e. one hour post-i.pl.
230 formalin injection), rats were deeply anesthetized with
231 25% urethane, then transcardially perfused with 0.1%
232 heparinized 0.1 M phosphate-buffered saline (PBS)
233 followed by ice cold 4% paraformaldehyde. A separate
234 group of rats ($n = 3$) received intraplantar injections of
235 saline (50 μ l) in lieu of formalin and were perfused
236 60 min later. Spinal cord tissue was extracted and kept
237 in the same fixative for 24 h and then cryoprotected in
238 30% sucrose for 3 days prior to sectioning.

Immunohistochemistry 239

240 Immunohistochemical experiments were conducted as
241 previously described (Tsou et al., 1996; Nackley et al.,
242 2003a,b; Carey et al., 2016). Transverse sections
243 (30 μ m) of the L4–L5 lumbar spinal cord were cut on a cryo-
244 stat and maintained in an antifreeze solution (50% sucrose
245 in ethylene glycol and 0.1 M PBS) prior to immunostaining.
246 Tissue was collected so that every fourth section would be
247 processed for immunohistochemistry to ensure that the
248 same cell could not be inadvertently counted twice in adja-
249 cent sections. Free-floating sections were washed three
250 times in 0.1 M PBS, and then immersed in 0.3% H₂O₂ for
251 30 min. To prevent non-specific binding, sections were pre-
252 treated for one hour with blocking buffer consisting of 5%
253 normal goat serum and 0.3% Triton X-100 in 0.1 M PBS,
254 followed by incubation with rabbit polyclonal Fos protein
255 antibody (1:1500, Santa Cruz Biotechnology, Dallas, TX,
256 USA) for 24 h at 4 °C. Fos-like immunoreactivity was visu-
257 alized using the avidin–biotin peroxidase method using
258 diaminobenzidine as the chromagen. Three sections per
259 animal displaying the highest levels of Fos-like immunore-
260 activity were selected and cells were counted from digitized
261 images using a Retiga 1300 digital camera and a Leica
262 DMLB microscope by an investigator blinded to the treat-
263 ment conditions. The number of FLI cells was counted in
264 each subdivision of the spinal cord as defined by Presley
265 et al. (1990) and averaged to produce a single mean for
266 each spinal cord region for each animal. Statistical analy-
267 ses were performed to compare the number of FLI cells
268 in each spinal cord region (averaged across animals, not
269 across sections) as described in our previously published
270 work (Tsou et al., 1996; Nackley et al., 2003a,b; Carey
271 et al., 2016; see also Fig. 1D). The subdivisions used were
272 the superficial laminae (laminae I and II), the nucleus pro-
273 prius (laminae III and IV), the neck of the dorsal horn (lami-
274 nae V and VI) and the ventral horn (laminae VII, VIII, IX,
275 and X) (Presley et al., 1990). Intraplantar injection of saline
276 in lieu of formalin ($n = 3$) did not induce appreciable
277 expression of Fos-like immunoreactivity, consistent with
278 the results of our previously published studies (Tsou
279 et al., 1996; Nackley et al., 2003a,b; Carey et al., 2016)
280 (data not shown).

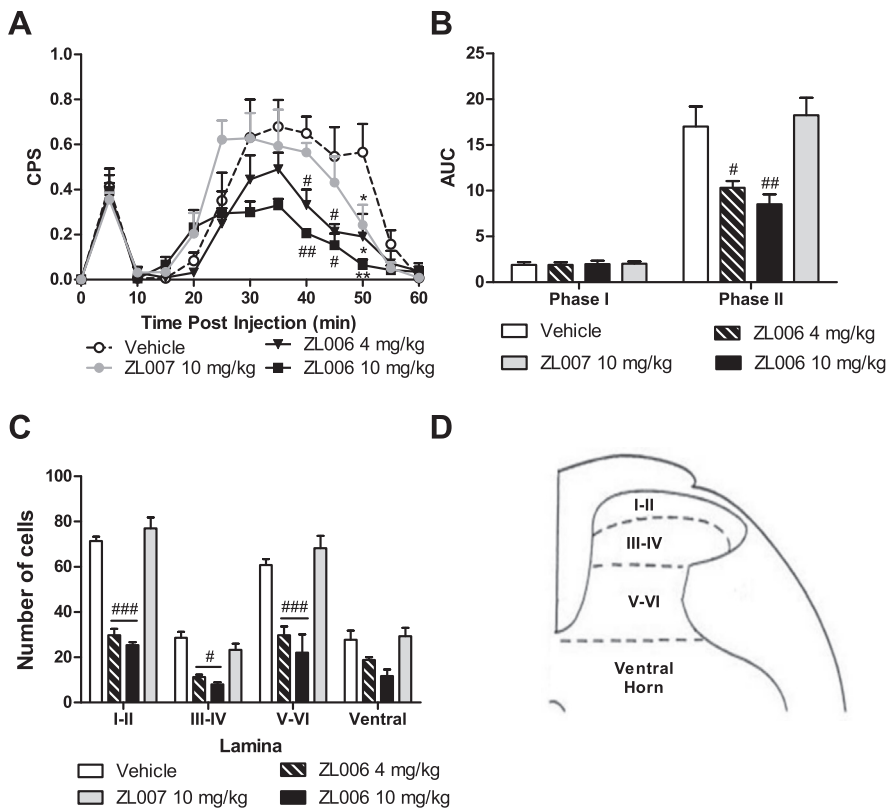


Fig. 1. ZL006 suppresses formalin-evoked nociceptive behavior and Fos-like immunoreactivity in lumbar spinal dorsal horn. (A) ZL006 (4 and 10 mg/kg i.p.) decreased composite pain scores (CPS) in a time-dependent manner. ZL006 (4 and 10 mg/kg i.p.) decreased formalin-induced CPS relative to ZL007 (10 mg/kg i.p.) and vehicle at 40 and 45 min post-formalin, while all groups showed lower CPS at 50 min post-formalin relative to vehicle. (B) ZL006 reduced the AUC of phase 2 but not phase 1 pain behavior relative to ZL007 and vehicle treatment. (C) ZL006 (4 and 10 mg/kg i.p.) decreased the number of Fos-like immunoreactive cells in the superficial dorsal horn, the nucleus proprius, and the neck region of the dorsal horn, whereas post hoc analyses did not reveal any differences between groups in the ventral horn. (D) Diagram of a lumbar spinal cord hemisection showing laminar subdivisions used to quantify formalin-evoked Fos protein expression (adapted from (Nackley et al., 2003b)). Data are expressed as mean \pm SEM ($n = 4-6$ per group). ### $p < 0.001$, ## $p < 0.01$, # $p < 0.05$ vs. ZL007 and vehicle; ** $p < 0.01$, * $p < 0.05$ vs. vehicle. One-way ANOVA Newman-Keuls post hoc. CPS: composite pain score, AUC: area under the curve.

single i.p. injection of ZL006 (2 or 4 mg/kg i.p.), ZL007 (4 mg/kg i.p.) or vehicle (i.p.). The highest dose of ZL006 evaluated in this study maximally suppressed formalin-evoked Fos protein expression and pain behavior and did not suppress Fos in the ventral horn. Mechanical and cold responsiveness were measured 30, 90 and 180 min post-drug.

Assessment of mechanical allodynia

Paw withdrawal thresholds to mechanical stimulation were measured using an electro von Frey anesthesiometer (IITC Life Science Inc., Woodland Hills, CA, USA) as described previously by our group (Rahn et al., 2008, 2014; Deng et al., 2012, 2016). Rats were placed on an elevated mesh platform underneath clear plastic observation chambers. Paw withdrawal thresholds were measured in duplicate in each paw, at each time point. Data are reported as the mean of these duplicate recordings averaged across paws.

Assessment of cold allodynia

Paw withdrawal frequencies to cold stimulation were measured using the acetone method as described previously by our group (Deng et al., 2012, 2016; Rahn et al., 2014). Rats were placed on an elevated mesh platform underneath clear plastic observation chambers, and a bubble of acetone was applied to the plantar surface of the hind paw using a blunt 1-ml syringe. Acetone was applied to each paw five times with 3 min intervals between stimulations. Animals were observed for 20 s after acetone application, and paw withdrawals were judged to be present if animals displayed one or more types of unilateral nocifensive behavior (licking, shaking, withdrawing, repetitive stepping on stimulated paw) during a given trial, whereas trials where animals did not display any form of unilateral nocifensive behavior were scored as zero. Paw withdrawal frequencies are reported as the percentage of trials wherein paw withdrawals occurred out of the 10 trials performed (5 trials per paw).

Generation of lumbar spinal cords for co-immunoprecipitation

A separate group of rats were treated with paclitaxel (2 mg/kg, i.p. on day 0, 2, 4 and 6 following initiation of paclitaxel dosing) or its cremophor-based vehicle and used to examine the impact of ZL006 versus vehicle treatment

Paclitaxel-induced peripheral neuropathic pain

Paclitaxel was used to produce chemotherapeutic-induced neuropathic pain in rats as described previously by our laboratory (Rahn et al., 2008, 2014; Deng et al., 2012, 2016). Rats were injected on four alternate days with paclitaxel (2 mg/kg, i.p.; cumulative dose 8 mg/kg i.p.) or its cremophor-based vehicle on day 0, 2, 4, and 6 following initiation of paclitaxel/cremophor vehicle dosing. The impact of small molecules and vehicle treatment on paclitaxel-induced mechanical and cold responsiveness was assessed during the maintenance phase of chemotherapy-induced neuropathy, when neuropathic pain was fully established, maximal and stable. We previously reported that paclitaxel-induced neuropathic pain is maximal and stable from day 12 post initiation of paclitaxel/cremophor vehicle dosing and was maintained throughout an 88-day observation interval (Deng et al., 2016). Following acquisition of baseline (pre-drug) levels of mechanical and cold responsiveness, rats received a

356 on co-immunoprecipitation of nNOS and PSD95 in the
357 lumbar spinal cord. Paclitaxel-treated rats were injected
358 (i.p.) with vehicle or ZL006 (10 mg/kg) during the
359 maintenance phase of chemotherapy-induced neuro-
360 pathic pain (i.e. day 16 following initiation of paclitaxel
361 dosing), when mechanical and cold hypersensitivity are
362 maximal (Deng et al., 2012, 2016; Rahn et al., 2014). Com-
363 parisons were made with a separate group of rats that
364 received the cremophor-based vehicle in lieu of paclitaxel
365 and was subsequently injected with the vehicle (i.e. day 16
366 following initiation of cremophor vehicle dosing on day 0, 2,
367 4 and 6). All rats were killed by rapid decapitation without
368 anesthesia 30 min post-injection of small molecule or vehi-
369 cle under identical conditions on the same day and were
370 not subjected to behavioral testing. Lumbar spinal cord tis-
371 sue was rapidly dissected and fast frozen in isopentane
372 and stored at -80°C until use.

373 Co-immunoprecipitation from spinal cord lysate 374 followed by immunoblotting

375 Lumbar spinal cord tissue was homogenized with low-salt
376 buffer (25 mM Tris-Cl, pH7.5, 70 mM NaCl, 1 mM EDTA,
377 pH 8.0, 1% Ipegal CA-630) supplemented with Halt
378 protease inhibitor cocktail and Halt phosphatase inhibitor
379 cocktail (ThermoFisher Scientific, Waltham, MA, USA),
380 and precleared at $13,000\text{ k}/4^{\circ}\text{C}$ for 10 min. nNOS
381 antibody at $1\text{ }\mu\text{g}$ per $100\text{ }\mu\text{g}$ of total protein lysate input
382 (Santa Cruz, Santa Cruz, CA, USA A-11) was added to
383 each lysate. Lysate-antibody mixtures were rotated for
384 one hour at 4°C . Magnetic protein G beads (Bio-rad,
385 Hercules, CA, USA) were then added, and rotated for
386 another 2 h. Beads were washed 5 times with the same
387 buffer, and drained beads were heated at 70°C for
388 10 min in LDS buffer for immunoblotting. All samples
389 were processed concurrently. Samples were loaded to
390 8% Bis-Tris Gel (ThermoFisher Scientific, Waltham, MA,
391 USA) and transferred to nitrocellulose membranes.
392 Nitrocellulose membranes were blocked with protein-
393 free blocking buffer (ThermoFisher Scientific, Waltham,
394 MA, USA) and incubated with mouse anti-nNOS (Santa
395 Cruz, Santa Cruz, CA, USA A-11, 1:10,000), rabbit anti-
396 PSD95 (ThermoFisher Scientific, Waltham, MA 700902,
397 USA, 1:1,000), rabbit anti-cofilin (Abcam, Cambridge,
398 UK, ab42824, 1:1000), and detected using goat anti-
399 rabbit-HRP (Santa Cruz, Santa Cruz, CA, USA,
400 1:10,000), and goat anti-mouse-HRP (Santa Cruz,
401 Santa Cruz, CA, USA, 1:10,000). Antibodies were
402 diluted in PBS-Tween 20 (0.05%) with 5% goat serum.
403 Blots were developed using SuperSignal West Femto
404 Maximum Sensitivity substrate (ThermoFisher Scientific,
405 Waltham, MA, USA) and visualized with a ChemiDoc
406 touch imaging system (Bio-rad, Hercules, CA, USA).
407 Images were quantified using Image Lab software (Bio-
408 rad, Hercules, CA, USA).

409 Data analysis

410 Data were analyzed by repeated measures Analysis of
411 Variance (ANOVA) and one-way ANOVA, as
412 appropriate. Post hoc comparisons were performed
413 using Newman-Keuls Post hoc test. Graphpad Prism

Version 5.02 statistical software for windows (GraphPad
Software, San Diego, CA, USA; www.graphpad.com)
was used to perform the aforementioned statistical
analyses. Statmate2 (GraphPad Software, San Diego,
CA, USA; www.graphpad.com) was used to calculate
statistical power of the co-immunoprecipitation
experiments using the sample sizes, standard deviations
and observed difference between group means.

422 RESULTS

423 ZL006 reduces formalin-evoked nociceptive behavior 424 and Fos-like immunoreactivity in spinal dorsal horn 425 regions associated with nociceptive processing

426 Intraplantar formalin increased CPS in a biphasic manner
427 ($F_{12,18} = 32.36$, $p < 0.0001$, Fig. 1A) in rats treated (i.p.)
428 with the PSD95-nNOS inhibitor ZL006, the putative
429 inactive analog ZL007 and vehicle. ZL006 treatment
430 decreased CPS ($F_{3,18} = 8.666$, $p < 0.001$, Fig. 1A), and
431 the interaction between time and drug treatment was
432 significant ($F_{36,18} = 2.512$, $p < 0.0001$, Fig. 1A). Post
433 hoc comparisons revealed that both the high (10 mg/kg
434 i.p.) and the low (4 mg/kg i.p.) dose of ZL006 decreased
435 phase 2 of formalin-induced pain behavior relative to
436 both ZL007 and vehicle treatments at 40 ($p < 0.01$,
437 0.05) and 45 min ($p < 0.05$) post-formalin. Pain scores
438 were higher in vehicle-treated rats compared to all other
439 groups at 50 min ($p < 0.05$ for each comparison) post-
440 formalin.

441 Formalin injection also increased the AUC of pain
442 behavior in a phase-dependent manner ($F_{1,38} = 209.4$,
443 $p < 0.0001$, Fig. 1B). ZL006 decreased the AUC of
444 formalin pain ($F_{3,38} = 9.044$, $p < 0.0001$, Fig. 1B)
445 selectively during phase 2 of nociceptive behavior
446 ($F_{3,38} = 8.931$, $p < 0.0001$, Fig. 1B). Both the low
447 ($p < 0.05$) and the high ($p < 0.01$) dose of ZL006
448 decreased the AUC of phase 2 pain behavior relative to
449 rats treated with vehicle or ZL007.

450 ZL006 decreased formalin-evoked Fos-like
451 immunoreactivity ($F_{2,36} = 110.3$, $p < 0.0001$, Fig. 1C) in
452 a lamina-dependent manner ($F_{3,36} = 48.55$, $p < 0.0001$,
453 Fig. 1C), and the interaction between drug and spinal
454 cord region was significant ($F_{6,36} = 7.602$, $p < 0.0001$,
455 Fig. 1C). Both the high and low doses of ZL006
456 decreased the number of formalin-evoked Fos-like
457 immunoreactive (FLI) cells relative to treatment with
458 vehicle or ZL007 in the superficial dorsal horn
459 ($p < 0.001$), the nucleus proprius ($p < 0.05$), and the
460 neck region of the dorsal horn ($p < 0.001$).
461 Pharmacological manipulations altered FLI cells in the
462 ventral horn ($p < 0.05$), but post hoc comparisons failed
463 to reveal significant differences between vehicle and
464 pharmacological treatments in the ventral horn. Example
465 photomicrographs are shown in Fig. 2.

466 IC87201 reduces formalin-evoked nociceptive 467 behavior and Fos-like immunoreactivity in spinal 468 dorsal horn regions associated with nociceptive 469 processing

470 Intraplantar administration of formalin increased CPS in a
471 biphasic manner ($F_{12,14} = 15.48$, $p < 0.0001$, Fig. 3A) in

472 rats receiving systemic injections of IC87201 or vehicle.
473 IC87201 reduced formalin-evoked nociceptive behaviors
474 ($F_{2,14} = 8.86$, $p < 0.01$, Fig. 3A), and the interaction
475 between time and IC87201 treatment was significant
476 ($F_{24,14} = 3.229$, $p < 0.0001$, Fig. 3A). Post hoc
477 comparisons revealed that the high dose of IC87201
478 (10 mg/kg i.p.) facilitated the onset (at 15 ($p < 0.05$)
479 and 20 min ($p < 0.01$)) and resolution (from 40–50 min
480 ($p < 0.05$ for each time point)) of formalin-induced pain
481 scores. The low dose of IC87201 (4 mg/kg i.p.) reliably
482 reduced formalin-evoked CPS at 45 ($p < 0.05$) minutes
483 post-formalin relative to vehicle.

484 Intraplantar (i.pl) formalin altered the AUC of formalin-
485 induced pain behavior in a phase-dependent manner in
486 these same subjects ($F_{1,28} = 110.2$, $p < 0.0001$,
487 Fig. 3B). IC87201 reduced the AUC of formalin pain
488 ($F_{2,28} = 6.536$, $p < 0.01$, Fig. 3B), selectively

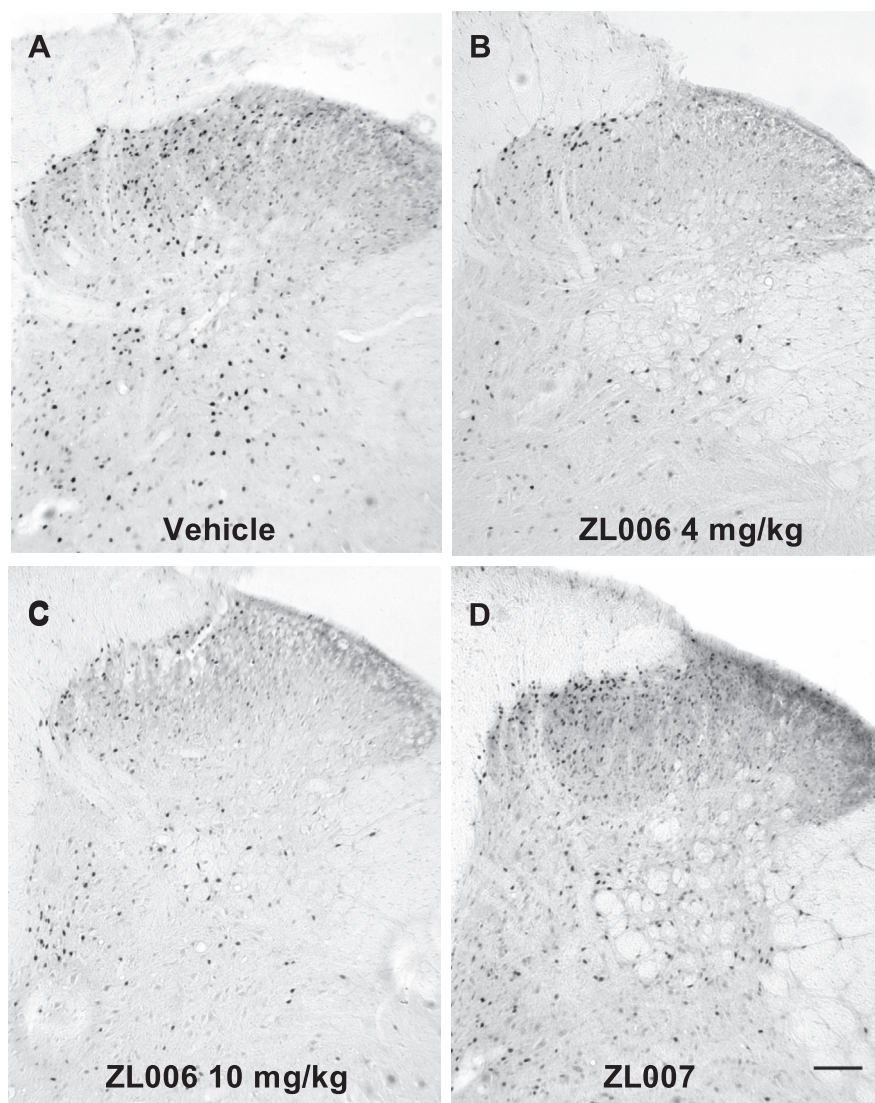
489 decreasing phase 2 pain behaviors ($F_{2,28} = 5.792$,
490 $p < 0.01$, Fig. 3B). Both the low and the high dose of
491 IC87201 decreased the AUC of phase 2 formalin pain
492 ($p < 0.05$ for each comparison) relative to vehicle-
493 treated rats. By contrast, the AUC of phase 1 formalin
494 pain did not differ between any of the treatment groups
495 ($p > 0.1$).

496 IC87201 also reduced formalin-evoked Fos-like
497 immunoreactivity ($F_{2,56} = 29.14$, $p < 0.0001$, Fig. 3C) in
498 a lamina-dependent manner ($F_{6,56} = 4.811$, $p < 0.001$,
499 Fig. 3C), and formalin also induced FLI in a lamina-
500 dependent manner ($F_{3,56} = 38.47$, $p < 0.0001$, Fig. 3C).
501 Both the low and high doses of IC87201 decreased
502 Fos-like immunoreactivity in the superficial dorsal horn
503 ($p < 0.0001$ for each dose). The high dose of IC87201
504 also reduced Fos-like immunoreactivity in the nucleus
505 proprius ($p < 0.05$) and the neck region of the dorsal
506 horn ($p < 0.05$). By contrast, the
507 number of FLI cells did not differ
508 between groups in the ventral horn
509 ($p > 0.4$).

509 Example
510 photomicrographs show the impact
511 of IC87201 treatment on formalin-
512 evoked FLI cells in Fig. 4.

513 IC87201 and ZL006 produce similar 514 levels of antinociception and 515 reductions of formalin-evoked 516 spinal Fos protein expression

517 We compared the efficacy of the
518 maximally efficacious doses of
519 IC87201 (10 mg/kg i.p.) and ZL006
520 (10 mg/kg i.p.) with the NMDAR
521 antagonist MK-801 (0.1 mg/kg) and
522 vehicle in suppressing formalin-
523 induced pain behavior and Fos-like
524 immunoreactivity. Formalin evoked a
525 biphasic pattern of nociceptive
526 behavior in these groups ($F_{12,19} =$
527 22.01 , $p < 0.0001$, Fig. 5A). Drug
528 treatment altered formalin-evoked
529 nociceptive behavior ($F_{3,19} = 14.93$,
530 $p < 0.0001$, Fig. 5A) in a time-
531 dependent manner ($F_{36,19} = 23.33$,
532 $p < 0.0001$, Fig. 5A). MK-801 and
533 IC87201 decreased CPS at 10 min
534 post-formalin relative to vehicle or
535 ZL006 ($p < 0.01$). Both PSD95–
536 nNOS inhibitors produced an
537 apparent leftward shift in the time
538 course of phase 2 pain behavior, as
539 revealed by facilitation of both the
540 onset and the resolution of pain
541 during this phase. IC87201 facilitated
542 the onset (from 15–20 min
543 post-formalin ($p < 0.05$)) and the
544 resolution of phase 2 pain (from
545 30–50 min post-formalin relative to
546 vehicle ($p < 0.05$)) behavior.
547 Similarly, ZL006 facilitated both the
548 onset (i.e. at 20 min post-formalin



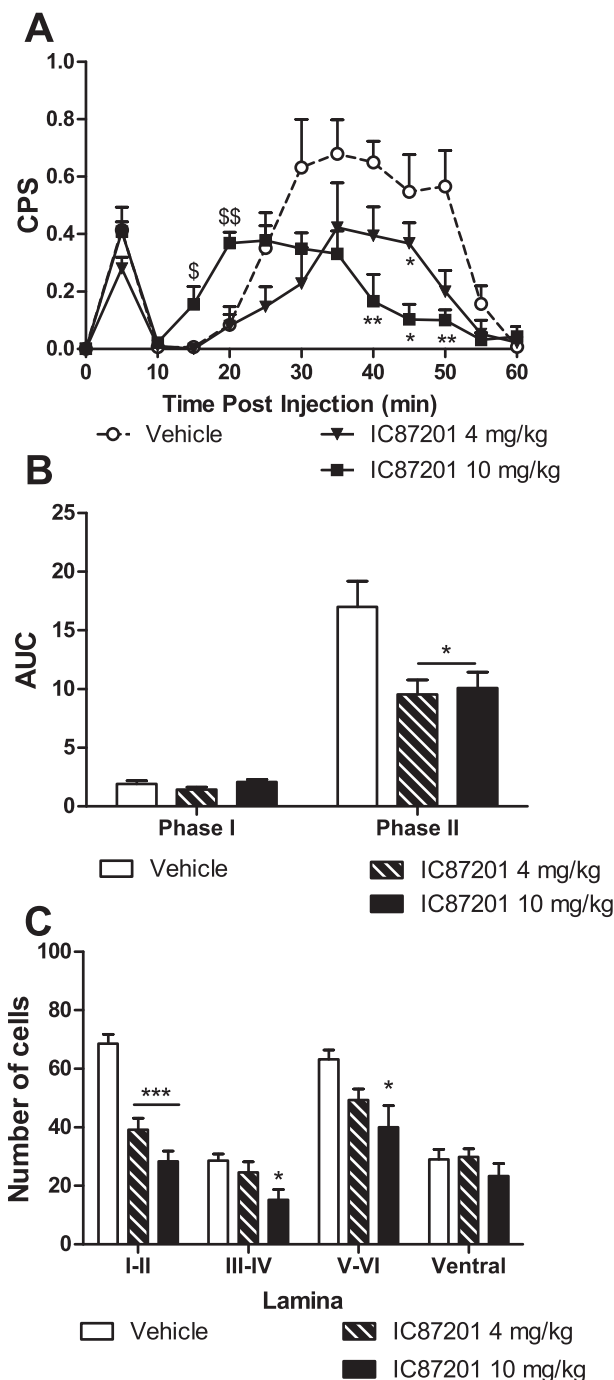
513 **Fig. 2.** Example photomicrographs taken at 10x magnification show formalin-evoked Fos-like
514 immunoreactive cells in lumbar dorsal horn of rats treated with vehicle (A), ZL006 (4 mg/kg i.p.)
515 (B), ZL006 (10 mg/kg i.p.) (C), and ZL007 (10 mg/kg i.p.) (D). Scale bar = 100 μ m. Fos protein
516 expression was largely absent in the dorsal horn contralateral to the formalin-treated paw. Fos
517 protein was not induced by intraplantar injection of saline (data not shown).

549 ($p < 0.05$) as well as the resolution of phase 2 (from 30–
550 50 min post formalin ($p < 0.05$) pain behavior. MK-801
551 reduced CPS at 25 min relative to all other groups
552 ($p < 0.05$). Effects of IC87201, ZL006 and MK801 did
553 not differ from each other at any other phase 2 time
554 point. MK-801 reliably suppressed pain behavior relative
555 to vehicle from 30–50 min post formalin ($p < 0.01$ for
556 each comparison).

557 Formalin increased the AUC of pain behavior in a
558 phase dependent manner ($F_{1,38} = 78.4$, $p < 0.0001$,
559 Fig. 5B). Drug treatment reduced the AUC
560 ($F_{3,38} = 14.42$, $p < 0.0001$, Fig. 5B) preferentially during

561 in phase 2 of formalin-evoked pain ($F_{3,38} = 13.15$,
562 $p < 0.0001$, Fig. 5B). ZL006 ($p < 0.01$) and IC87201
563 ($p < 0.05$) and MK-801 ($p < 0.001$) all reduced the
564 AUC of phase 2 formalin-evoked pain relative to vehicle
565 whereas MK-801 produced a greater suppression of the
566 AUC of phase 2 pain behavior relative to IC87201 and
567 ZL006 ($p < 0.05$).

568 Treatment with either IC87201, ZL006 or MK-801 also
569 reduced the number of formalin-evoked Fos protein-like
570 immunoreactive cells ($F_{3,76} = 70.37$, $p < 0.0001$,
571 Fig. 5C) in a lamina-dependent manner ($F_{9,76} = 6.261$,
572 $p < 0.0001$, Fig. 5C) and the number of FLI cells also
573 differed as a function of spinal cord region
574 ($F_{3,76} = 32.82$, $p < 0.0001$, Fig. 5C). IC87201
575 ($p < 0.01$), ZL006 ($p < 0.01$) and MK-801 ($p < 0.001$)
576 reduced formalin-evoked Fos protein expression relative
577 to vehicle in the superficial dorsal horn, the nucleus
578 proprius and the ventral horn. MK-801 produced a
579 greater suppression of the number of FLI cells relative
580 to IC87201 and ZL006 in the superficial dorsal horn and
581 neck region of the dorsal horn ($p < 0.01$ for each
582 comparison). In the ventral horn, only MK-801
583 ($p < 0.01$) reliably reduced formalin-evoked Fos-like
584 immunoreactivity relative to vehicle. Example
585 photomicrographs show the impact of maximally
586 efficacious doses of PSD95–nNOS inhibitors ZL006 and
587 IC87201 and the NMDAR antagonist MK-801 on
588 formalin-evoked Fos protein expression in the lumbar
589 dorsal horn (Fig 6).



ZL006 and IC87201 do not impair motor performance in the rotarod test in rats, whereas MK-801 induces motor ataxia

590 Rotarod performance did not differ between groups prior
591 to pharmacological manipulations (baseline) ($p > 0.5$).
592 MK-801 reduced the rotarod descent latency
593 ($F_{3,18} = 3.07$, $p \leq 0.05$, Fig. 7) at 30 min post-injection
594 relative to vehicle ($p < 0.05$) and relative to all other
595 groups ($F_{3,18} = 3.604$, $p < 0.05$, Fig. 7) at 60 min post
596 injection. The PSD95–nNOS inhibitors ZL006 and
597 IC87201 did not impair rotarod performance in rats at
598 any time point.
599
600
601

Fig. 3. IC87201 suppresses formalin-evoked nociceptive behavior and Fos-like immunoreactivity in lumbar spinal dorsal horn. IC87201 differentially altered the time course of formalin-induced composite pain scores. IC87201 (10 mg/kg i.p.) facilitated the onset of CPS 15–20 min post-formalin relative to all other groups and enhanced resolution of phase 2 pain behavior; CPS were reduced by IC87201 from 40–50 min post-formalin relative to vehicle treated-rats (A). IC87201 (4 mg/kg i.p.) reduced formalin-evoked CPS at 45 min post-injection relative to vehicle (A). IC87201 (4 and 10 mg/kg i.p.) reduced the AUC of phase 2 formalin-evoked pain (B). IC87201 (4 and 10 mg/kg i.p.) reduced the number of Fos-like immunoreactive cells in the superficial dorsal horn, whereas only the high dose reduced Fos protein expression in the nucleus proprius and the neck region of the dorsal horn (C). Data are expressed as mean \pm SEM ($n = 5–6$ per group). $^{ss}p < 0.01$, $^sp < 0.05$ IC87201 10 mg/kg vs. all other groups; $^{***}p < 0.001$, $^{**}p < 0.01$, $^*p < 0.05$ vs. vehicle. One-Way ANOVA, Newman-Keuls post hoc. CPS: composite pain score, AUC: area under the curve.

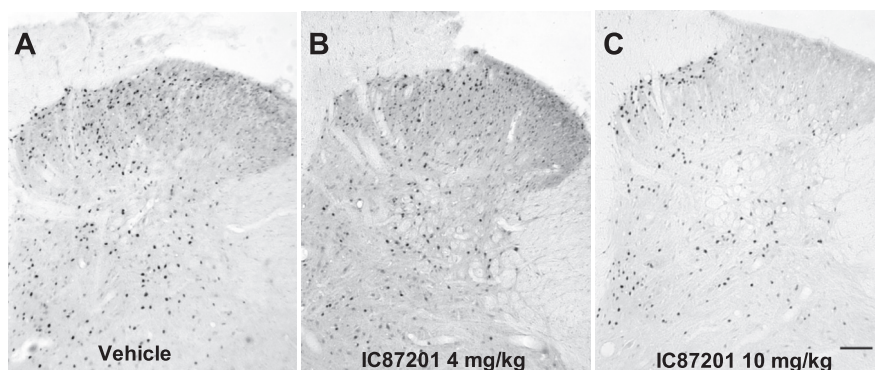


Fig. 4. Example photomicrographs taken at 10x magnification show formalin-evoked Fos-like immunoreactive cells in lumbar dorsal horn of rats treated with vehicle (A), IC87201 (4 mg/kg i.p.) (B) and IC87201 (10 mg/kg i.p.) (C). Scale bar = 100 μ m. Fos protein expression was largely absent in the dorsal horn contralateral to the formalin-treated paw.

ZL006 reduces paclitaxel-induced mechanical and cold allodynia in rats

Paclitaxel produced mechanical ($F_{3,66} = 27.22$, $p < 0.0001$; Fig. 8A) and cold allodynia ($F_{3,66} = 34.15$, $p < 0.0001$; Fig. 8B) that was differentially impacted by ZL006, ZL007 and vehicle treatment. ZL006 reduced paclitaxel-induced mechanical hypersensitivity ($F_{3,66} = 29.48$, $p < 0.0001$; Fig. 8A), and the interaction was significant ($F_{9,66} = 11.43$, $p < 0.0001$; Fig. 8A). The high dose of ZL006 (4 mg/kg i.p.) elevated mechanical paw withdrawal thresholds at 30 min post-injection relative to all other groups ($p < 0.001$). ZL006 remained efficacious in producing antinociception at 90 min post-injection relative to rats treated with ZL007 (4 mg/kg i.p.) and vehicle (i.p.) ($p < 0.001$). The low dose of ZL006 (2 mg/kg i.p.) elevated mechanical paw withdrawal thresholds at 30 ($p < 0.01$), 90 ($p < 0.05$), and 180 ($p < 0.05$) minutes post injection relative to rats treated with ZL007 (4/mg/kg) or vehicle. ZL006 also decreased cold allodynia ($F_{3,66} = 17.35$, $p < 0.0001$; Fig. 8B), and the interaction was significant ($F_{9,66} = 13.67$, $p < 0.0001$; Fig. 8B). The high dose of ZL006 (4 mg/kg i.p.) reduced the frequency of withdrawing to the acetone-stimulated paw at 30 ($p < 0.001$) and 90 ($p < 0.05$) minutes post-injection relative to ZL007- (4 mg/kg i.p.) and vehicle-treated rats. The low dose of ZL006 (2 mg/kg i.p.) reduced paclitaxel-induced cold responsiveness at 30 ($p < 0.001$) minutes post-injection relative to ZL007- and vehicle-treated rats.

The PSD95/nNOS complex is present in the lumbar spinal cord of paclitaxel-treated rats

Paclitaxel produced mechanical hypersensitivity ($F_{1,10} = 377.4$, $p < 0.0001$; Fig. 9A) that was dependent upon the treatment phase ($F_{1,10} = 213.8$, $p < 0.0001$; Fig. 9A), and the interaction was significant ($F_{1,10} = 196.1$, $p < 0.0001$; Fig. 9A). While neither group differed at baseline ($p > 0.6$), paclitaxel decreased mechanical paw withdrawal thresholds relative to rats treated with cremophor-based vehicle ($t_{10} = 18.72$, $p < 0.0001$; Fig. 9A). PSD95 and nNOS proteins and the nNOS/PSD95 complex were also

present in the lumbar spinal cord (Fig. 9B). However, paclitaxel did not reliably increase association of PSD95 with nNOS in the lumbar spinal cord tissue ($p > 0.2$, one-tailed t -test). ZL006 ($p = 0.19$, one-tailed t -test) did not reliably reduce levels of nNOS/PSD95 interaction in lumbar spinal cord relative to vehicle treatment in paclitaxel-treated rats in all subjects. The observed power of the nonsignificant unpaired t -test comparing impact of ZL006 versus vehicle treatment on the association of PSD95 and nNOS in paclitaxel-treated lumbar spinal cords was 20%. A sample size of 30 per group would be required to detect a ZL006-induced disruption of PSD95–NOS

association based upon the observed standard deviation, sample size and magnitude difference between means.

DISCUSSION

NMDARs are a critical link in the development and maintenance of central sensitization (Woolf and Thompson, 1991). NMDAR-mediated production of NO is of particular importance mechanistically as an effector pathway in the generation of persistent pathological pain (Meller and Gebhart, 1993). Therefore, reducing NMDAR-mediated production of NO represents a promising mechanism to alleviate chronic pain conditions. However, the problematic side effects associated with direct NMDAR antagonists and NOS inhibitors indicate the need for alternate mechanisms to suppress NMDAR-dependent NO production (Rees et al., 1989; Kobayashi et al., 1991; Bohme et al., 1993; Krystal et al., 1994; Holscher et al., 1996; Pal et al., 2002; Rickard and Gibbs, 2003; Koylu et al., 2005; Yildiz Akar et al., 2007). Because the scaffolding protein PSD95 tethers nNOS to NMDARs, protein–protein interactions between PSD95 and nNOS are required for NMDAR-mediated production of NO (Sattler et al., 1999). We, therefore, hypothesized that selective disruption of PSD95–nNOS protein–protein interactions would suppress CNS sensitization associated with pathological pain without the unwanted side effects of NMDAR antagonists. Our studies using the formalin test suggest that putative small molecule inhibitors of the protein–protein interaction between PSD95 and nNOS suppress NMDAR-dependent pain behavior as well as inflammation-evoked neuronal activation in the spinal dorsal horn without unwanted side effects of NMDAR antagonists.

In the present work, two pharmacological inhibitors of PSD95–nNOS protein–protein interactions, IC87201 and ZL006, selectively suppressed both formalin-evoked activation of spinal dorsal horn neuronal circuitry and formalin-evoked pain behavior in the same subjects. In our study, IC87201 and ZL006, but not the inactive analog ZL007, reduced formalin-evoked pain behavior

702 and Fos protein expression in the lumbar dorsal horn.
703 These observations are important because they support
704 the hypothesis that antinociceptive effects of
705 PSD95–nNOS inhibitors reflect a suppression of
706 nociceptive processing at the level of the CNS.
707 Moreover, PSD95–nNOS inhibitors selectively

708 suppressed phase 2 of formalin pain, which is
709 specifically linked to CNS sensitization (Hylden et al.,
710 1989; Lebrun et al., 2000), similar to the NMDAR antago-
711 nist MK-801. Phase 1 of formalin pain, which has been
712 linked closely to primary afferent activation (Puig and
713 Sorkin, 1996), was unaffected by PSD95–nNOS inhibi-
714 tors. Moreover, we show that both ZL006 and IC87201,
715 administered systemically, produced antinociception in
716 rats whereas ZL007 was ineffective. Similarly, at the dose
717 that maximally reduced formalin-evoked nociceptive
718 behavior and Fos protein expression, ZL006, which has
719 not previously shown efficacy in rats in any prior publica-
720 tion, reduced paclitaxel-induced mechanical and cold
721 hypersensitivity whereas ZL007 was ineffective. Our
722 study is the first to demonstrate that the small molecule
723 protein–protein interaction inhibitor ZL006 produces
724 antinociception in rats. ZL006, has been reported to exhibit
725 limited blood–brain barrier penetration (Wang et al.,
726 2015) but efficacy exhibited by this compound in models
727 of post-traumatic stress disorder (Shekar et al., 2012)
728 and depression (Doucet et al., 2013) argue for central
729 sites of action of ZL006. By contrast, ZL007 was ineffec-
730 tive in suppressing either formalin-evoked pain behavior
731 or formalin-evoked Fos protein expression in rats. This
732 observation is noteworthy because ZL007 failed to disrupt
733 co-immunoprecipitation of nNOS and PSD95 in mouse
734 hippocampal slice cultures observed with ZL006 (Zhou
735 et al., 2010) but disrupted binding between purified
736 PSD95 and nNOS interactions in our Alphascreen bio-
737 chemical assay (unpublished data). The present study
738 extends previous reports from our lab indicating that
739 IC87201 and ZL006 specifically disrupt the interaction
740 between purified nNOS and PSD95 proteins *in vitro*,
741 reduce glutamate-induced excitotoxicity in cultured cortical
742 neurons, and produce antinociceptive efficacy in
743 mouse models of inflammatory and neuropathic pain in

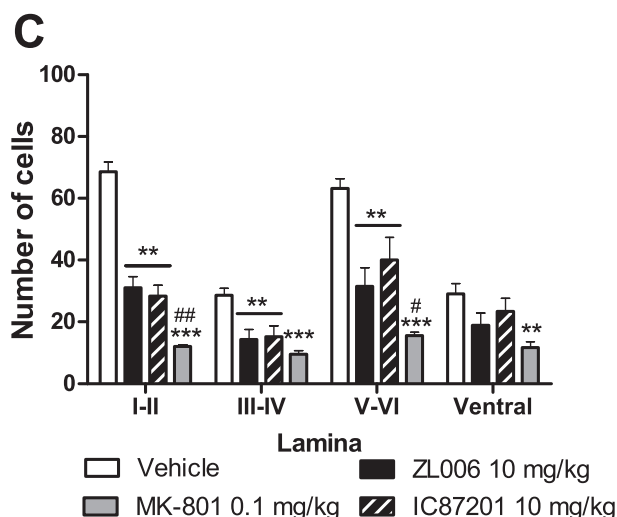
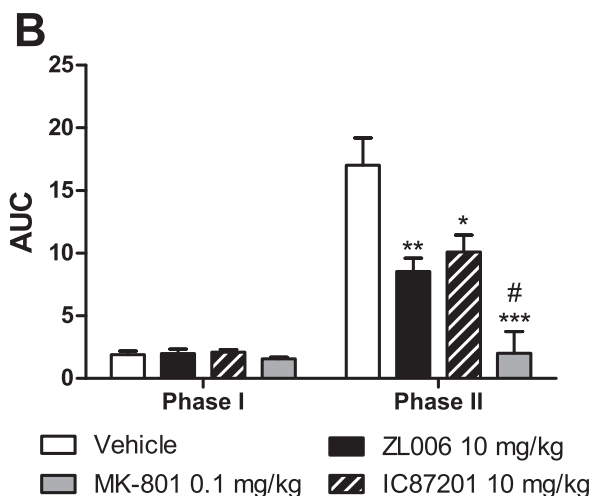
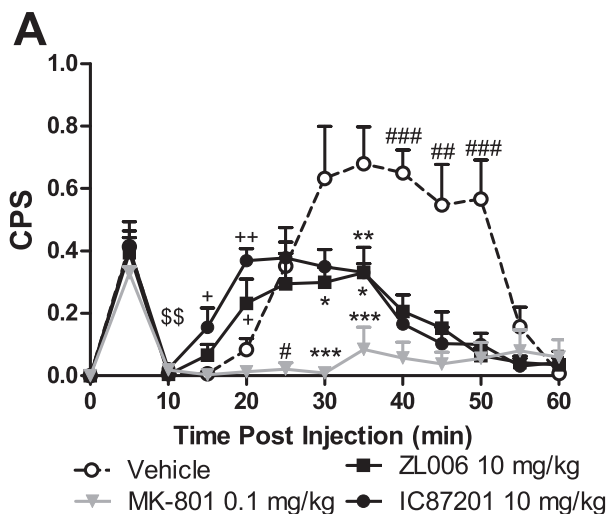


Fig. 5. ZL006 and IC87201 produce comparable suppressions of formalin-evoked pain behavior and Fos-like immunoreactivity in spinal dorsal horn. IC87201 decreased composite pain scores at 10 min post-formalin relative to rats treated with ZL006 or vehicle. IC87201 facilitated the onset (15–20 min) of formalin-induced CPS relative to vehicle or MK-801 treatment as well as the resolution of phase 2 pain (decreasing CPS from 40–50 min post-formalin) relative to vehicle (A). ZL006-treated rats displayed a transient increase in CPS at 20 minutes post-formalin relative to rats treated with MK-801 or vehicle, and decreased CPS at 30–50 minutes post-formalin relative to vehicle-treated rats (A). MK-801 reduces AUC relative to all groups, whereas ZL006 and IC87201 reduce the AUC of phase 2 formalin pain relative to vehicle (B). ZL006, IC87201 and MK-801 reduced Fos-like immunoreactivity in the superficial dorsal horn, the nucleus proprius, and the neck region of the dorsal horn relative to vehicle (C). MK-801 produced a greater suppression of the number of FLI cells relative to ZL006 and IC87201 in the superficial dorsal horn and the neck region of the dorsal horn (C). Only MK-801 reliably suppressed the number of FLI cells in the ventral horn (C). Data are expressed as mean ± SEM ($n = 5–6$ per group). $^{*}p < 0.01$, $^{+}p < 0.05$ vs. vehicle and MK-801; $^{**}p < 0.001$, $^{***}p < 0.01$, $^{*}p < 0.05$ vs. vehicle; $^{###}p < 0.001$, $^{##}p < 0.01$, $^{#}p < 0.05$ vs. all other groups. One-way ANOVA, Newman–Keuls post hoc. CPS: composite pain score, AUC: area under the curve.

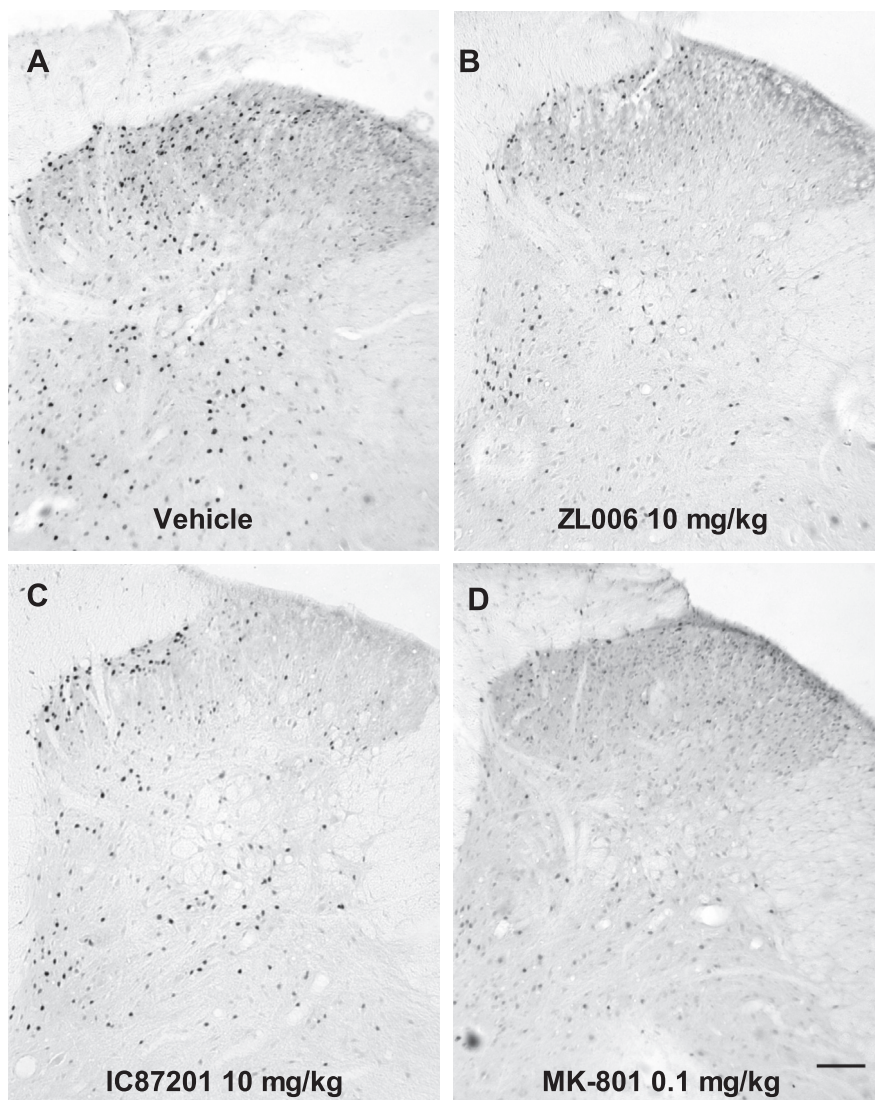


Fig. 6. Example photomicrographs taken at 10x magnification showing formalin-evoked Fos-like immunoreactive cells in lumbar dorsal horn of rats treated with vehicle (A), ZL006 (10 mg/kg i.p.) (B), IC87201 (10 mg/kg i.p.) (C), or MK-801 (0.1 mg/kg) (D). Scale bar = 100 μ m. Fos expression was largely absent in the dorsal horn contralateral to the formalin-treated paw

mice (Lee et al., 2015). We previously verified that both IC87201 and ZL006 suppress NMDA-stimulated cGMP formation, a marker of NO production, in cultured hippocampal neurons (Smith et al., 2016). Thus, we have used validated pharmacological tools to test the hypothesis that PSD95–nNOS inhibitors suppress formalin-evoked neuronal activation and pain behavior *in vivo* using the same subjects. Nonetheless, caution must be exerted in extrapolating effects of ZL007 from *in vitro* to *in vivo* levels and/or across species (mice vs. rats). Moreover, because we evaluated a clinically relevant systemic route of drug administration more work is necessary to determine the site of action of small molecule PSD95–nNOS inhibitors by using intrathecal, intraventricular and site-specific intracranial injections in multiple brain regions. The observed pattern of antinociceptive efficacy during phase 2 (but not phase 1) of formalin pain, and in suppressing formalin-evoked protein expression, is

consistent with suppression of CNS sensitization by PSD95–nNOS inhibitors.

Our studies also demonstrated that the putative PSD95–nNOS inhibitor ZL006, but not the inactive analog ZL007, suppressed mechanical and cold allodynia induced by treatment with the chemotherapeutic agent paclitaxel. We, therefore, examined whether the association of nNOS and PSD95 was increased in the lumbar spinal cord during the maintenance phase of paclitaxel-induced neuropathic pain at a time point when ZL006, but not ZL007, produced antinociception. ZL006 was specifically used for our studies because this ligand was shown previously to spare NMDAR subunit NR2B-PSD95 interactions (Zhou et al., 2010) and a structurally similar inactive analog (ZL007) was synthesized by us to confirm specificity of mechanism of action. Zhou et al. (2010) previously reported that the association of nNOS and PSD95 is increased in brain tissue in rodent models of cerebral ischemia and was disrupted by ZL006 with sample sizes of three per group. Paclitaxel, rather than unilateral formalin injection, was used for our co-immunoprecipitation studies because toxic challenge with a systemically administered chemotherapeutic agent can be expected to impact the spinal cord bilaterally rather than unilaterally and insufficient protein levels in native tissue would be expected to limit sensitivity of the detection method in dorsal horn hemisections derived from formalin-treated rats. While treatment with the chemotherapeutic agent paclitaxel produced allodynia, a reliable increase in the association of nNOS and PSD95 during the maintenance phase of paclitaxel-induced neuropathic pain (i.e. 16 days following onset of treatment) was not observed in lumbar spinal cord tissue using our validated co-immunoprecipitation methods. More work is necessary to determine whether supraspinal sites of antinociceptive action and descending mechanisms could contribute to the pattern of antinociceptive efficacy and results obtained here. Our studies, nonetheless, provide the important demonstration that ZL006, but not ZL007, attenuated both mechanical and cold hypersensitivity induced by paclitaxel treatment in rats, confirming utility of ZL007 as an inactive analog for *in vivo* manipulations in rats. However, while systemic treatment (i.p.) with ZL006 decreased the association of nNOS and PSD95 in paclitaxel-treated rats relative to paclitaxel-treated rats

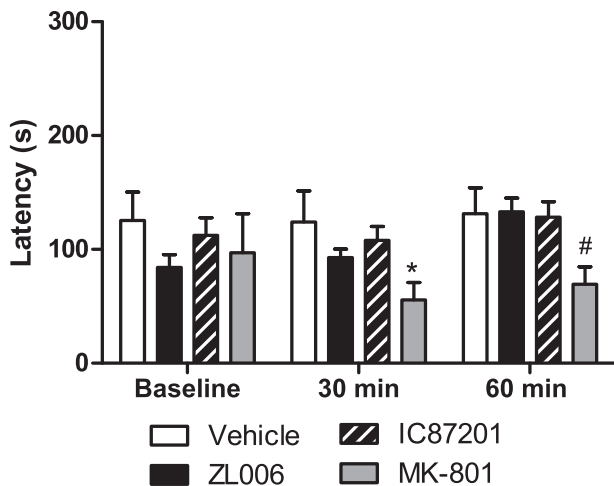


Fig. 7. The NMDAR antagonist MK-801 impairs rotarod performance in rats whereas PSD95–nNOS inhibitors ZL006 and IC87201 do not. MK-801 reduced descent latency in the rotarod test at 30 min post-injection relative to vehicle and 60 min post-injection relative to all other groups. ZL006 and IC87201 did not impair rotarod performance. Data are expressed as mean \pm SEM ($n = 5–6$ per group). * $p < 0.05$ vs. vehicle; # $p < 0.05$ vs. all other groups. One-way ANOVA, Newman–Keuls post hoc.

823 receiving vehicle (i.p.), this reduction failed to reach statistical significance. The failure to observe a reliable decrease in the association of nNOS and PSD95 in the present co-immunoprecipitation experiments could be attributed to a number of factors. Power analyses performed on the data derived from our paclitaxel-treated spinal cords indicate that our study was underpowered to detect significant mean differences between ZL006 and vehicle treatment, with observed power being only 20%. Moreover, large sample sizes ($n = 30$ per group) would be necessary to achieve 80% power to detect the observed 0.28 magnitude difference between means with alpha set at 0.05. The previous report by Zhou et al. demonstrating that ZL006 disrupts nNOS-PSD95 association *in vivo* used a different route of administration (i.v. vs. i.p.), a different tissue type (mouse cortex vs. rat lumbar spinal cord), and a more robust model of pathology (middle cerebral arterial occlusion vs. chemotherapy-induced neuropathic pain). Moreover, because the entire lumbar spinal cord (i.e. including dorsal and ventral horn and surrounding white matter), was processed to ensure uniformity of samples between subjects, it is also possible that the sampling methods employed may have diluted the magnitude of observed changes and sensitivity of the methods used to detect disruption of the PSD95–nNOS complex. Because PSD95 binds many proteins, it is also possible that ubiquity of PSD95 relative to nNOS may limit ability to detect changes in the PSD95–nNOS complex by co-ip. It is also possible that changes in downstream signaling can occur with only transient changes in the PSD95–nNOS complex. Finally, supraspinal as well as spinal sites of action could contribute to the antinociceptive effects of systemically administered PSD95–nNOS inhibitors. Such factors could limit the ability to detect robust increases in the PSD95–nNOS complex and a reliable decrease in their association produced by

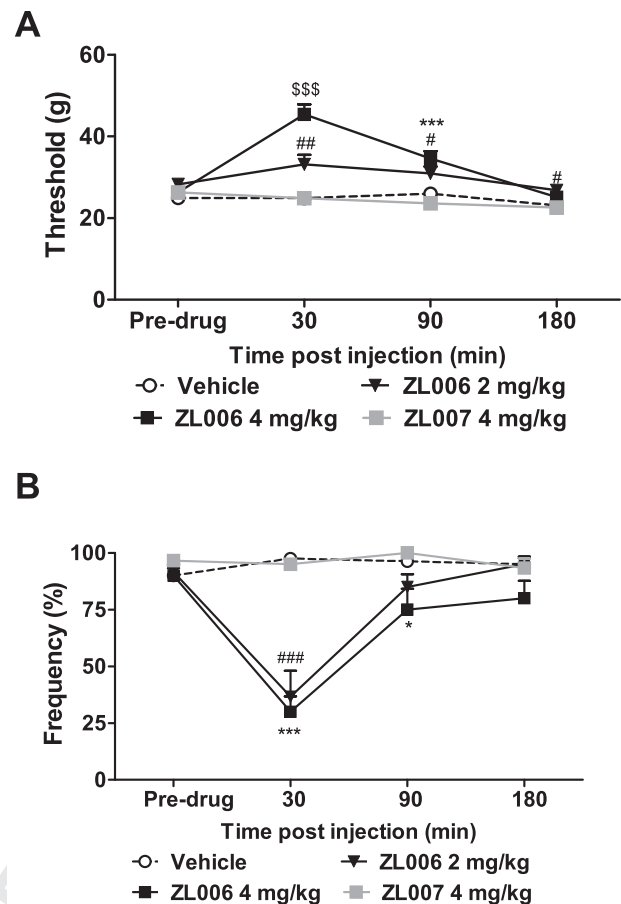


Fig. 8. ZL006 attenuates paclitaxel-induced mechanical and cold allodynia. ZL006 (4 mg/kg i.p.) increased the threshold for paw withdrawal to mechanical stimulation in paclitaxel-treated rats relative to vehicle and ZL007 (4 mg/kg i.p.) treatment at 30 and 90 min post-injection. The high dose of ZL006 produced a greater antinociceptive effect compared to the low dose of ZL006 at 30 min post-injection (A). ZL006 (2 mg/kg i.p.) reduced mechanical hypersensitivity at 30, 90 and 180 min post-injection relative to rats treated with ZL007 or vehicle (A). In paclitaxel-treated rats, ZL006 (2 mg/kg i.p.) reduced the frequency of paw withdrawal to cold stimulation (cold allodynia) at 30 min post-injection relative to ZL007- and vehicle-treated rats (B). ZL006 (4 mg/kg i.p.) reduced cold allodynia at 30 and 90 min post-injection relative to ZL007 (4 mg/kg i.p.) and vehicle (B). Data are expressed as mean \pm SEM ($n = 6–8$ per group). \$\$\$ $p < 0.001$ ZL006 4 mg/kg vs. all other groups; *** $p < 0.001$, * $p < 0.05$ ZL006 4 mg/kg vs. ZL007 and vehicle; ### $p < 0.001$, ## $p < 0.01$, # $p < 0.05$ ZL006 2 mg/kg vs. ZL007 and vehicle. Two-way ANOVA, one-way ANOVA, Newman–Keuls post hoc.

ZL006 treatment in lumbar spinal cord. Additional work is necessary to evaluate the site of action of PSD95–nNOS inhibitors and to determine whether other CNS regions (i.e. punches derived from yet to be identified brain regions) provide adequate protein levels for the detection of the PSD95–nNOS complex and determine whether other pathological pain states produce a measurable increase in the association of nNOS and PSD95 and. Nonetheless, it is important to emphasize that the PSD95–nNOS complex was reliably detected in lumbar spinal cord of paclitaxel-treated rats. Moreover, ZL006 was effective at reducing the behavioral manifestations of two mechanistically distinct types of pain, as well as in suppressing noxious stimulus-evoked neuronal

873 activation within spinal dorsal horn nociceptive circuitry,
874 whereas ZL007 was inactive under the same conditions.
875 Formalin-evoked nociceptive behavior occurs in two
876 distinct phases, with an immediate primary nocifensive
877 phase lasting 0–5 min thought to reflect primary afferent
878 activation (Puig and Sorkin, 1996), and a second phase
879 beginning 15–20 min post-formalin injection, which is
880 thought to reflect sensitization occurring within the spinal

cord and facilitation of responses to otherwise innocuous
stimulation (Hylden et al., 1989; Lebrun et al., 2000). The
time period between phases of formalin-evoked pain (i.e.
5–15 min post-injection) is normally characterized by a
state of quiescence and disappearance of nociceptive
behavior attributed to transient reductions in activity of pri-
mary afferent nociceptors (Puig and Sorkin, 1996) and
descending inhibitory controls (Franklin and Abbott,
1993; Kaneko and Hammond, 1997). Both doses of
IC87201 and ZL006 reduced overall nocifensive behavior
in the second phase of formalin-evoked pain in rats, as
demonstrated by quantification of the AUC of phase 2
pain behavior. However, IC87201, and to a lesser extent,
ZL006 also produced an apparent leftward shift in both
the onset and resolution of phase 2 nociceptive behav-
iors. While NO is typically thought of as a proinflammatory
mediator, differences in peripheral vs. central activity of
NO exist could account for this effect. NOS inhibitors have
been reported to exacerbate and prolong the resolution of
inflammation when administered locally to sites of inflam-
mation, whereas systemic administration of these agents
attenuated inflammation (Paul-Clark et al., 2001). NO
modulates neuronal function at spinal and supraspinal
sites in a complex manner (see Prast and Philippu,
2001 for review). It is possible that the apparent increase
in pain observed in animals treated with the highest doses
of IC87201 and ZL006 during the interphase pain reflects
a leftward shift in the onset of phase 2 pain behavior that
could have occurred due to modulation of descending
inhibitory control circuitry. It is important to note that while
both the onset and the resolution of phase 2 pain behavior
was facilitated by PSD95–nNOS inhibitors, the total
amount of phase 2 pain behavior, as defined by the AUC,
was markedly diminished by PSD95–nNOS inhibitor
treatment with either active analog. Likewise, all com-
pounds were administered systemically, and PSD95–nNOS
inhibitors would, hypothetically, only target postsynaptic
neurons that contain NMDARs, PSD95 and nNOS. Thus,
NOS inhibitors, which nonspecifically inhibit nNOS as well
as endothelial nitric oxide synthase (eNOS), (see Vitecek
et al., 2012 for review) could be expected to produce a
different pattern of *in vivo* effects on nociceptive respond-
ing. For example, NOS inhibitors or NO application can
produce pro- or antinociceptive effects varying with local
vs. systemic application by altering peripheral nociceptive
responding while lowering

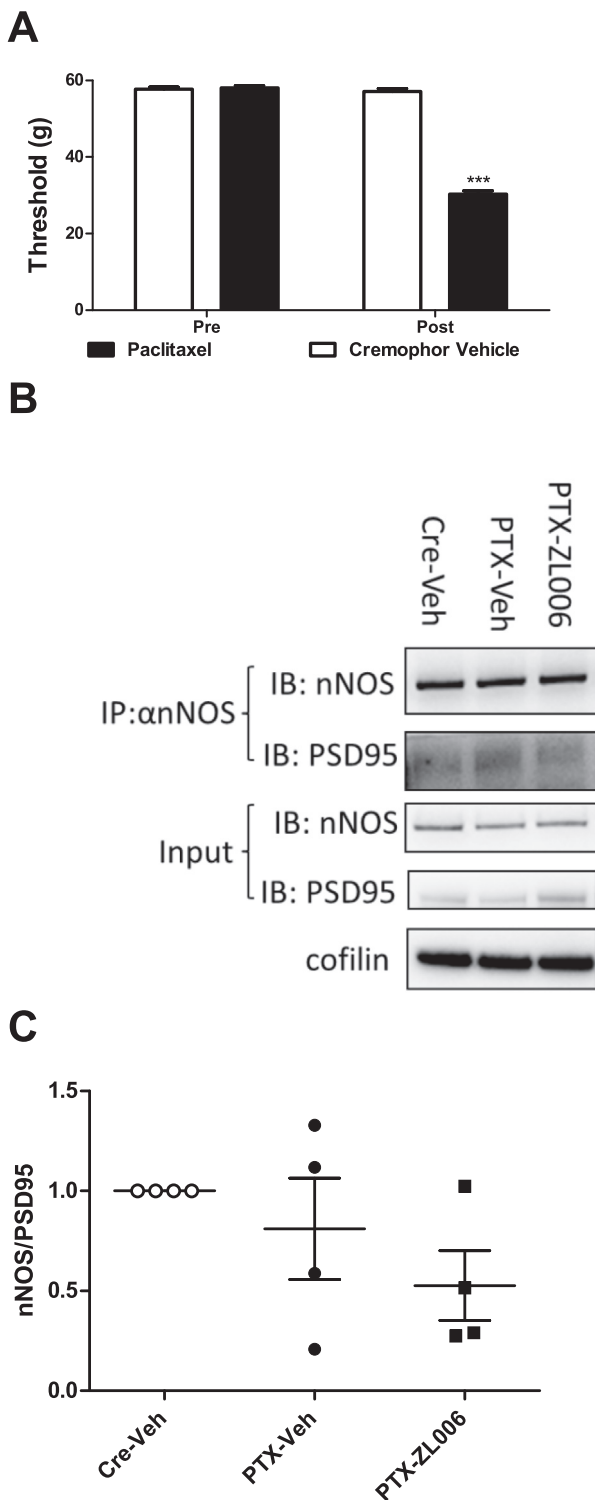


Fig. 9. The PSD95–nNOS complex is present in the spinal cord of the paclitaxel-treated rats. Paclitaxel treatment decreased paw withdrawal thresholds to mechanical stimulation relative to rats treated with cremophor-based vehicle and relative to pre-injection baseline responding (A). Data are mean ± SEM ($n = 4–8$ per group). *** $p < 0.0001$ paclitaxel-treated rats vs. cremophor-treated rats. Two-way ANOVA, two-tailed paired t-test. Representative western blots showing coimmunoprecipitation of PSD95 with nNOS in the lumbar spinal cord of rats treated with either paclitaxel (PTX) or cremophor-based vehicle (B). Paclitaxel treatment did not reliably alter the association of nNOS and PSD95 in lumbar spinal cord (C). nNOS/PSD95 levels in cremophor-treated rats receiving vehicle (Cre-Veh) and paclitaxel-treated rats receiving vehicle (PTX-Veh) or ZL006 (10 mg/kg i.p.) (PTX-ZL006) (C). Data are mean ± SEM with scatterplot showing individual subjects data ($n = 4$ per group).

927 central sensitization driven by peripheral nociceptors.
928 Presumably, PSD95–nNOS protein–protein interaction
929 inhibitors require interaction with postsynaptic proteins
930 (i.e. PSD95) that would specifically alter CNS sensitiza-
931 tion. Future studies could examine whether PSD95–
932 nNOS protein–protein interaction inhibitors lack efficacy
933 following local injections in the hind paw that would target
934 peripheral mechanisms. Nonetheless, both IC87201 and
935 ZL006 were effective overall at reducing pain behaviors
936 *throughout* the second phase of formalin-evoked pain in
937 its entirety. ZL007, an analog of ZL006, failed to produce
938 antinociceptive efficacy in rats in the current study, and,
939 likewise, failed to decrease formalin-evoked Fos-like
940 immunoreactivity in lumbar spinal dorsal horn. While
941 ZL006, IC87201 and MK-801 all effectively reduced pain
942 behavior in phase 2 of formalin-evoked pain and
943 Fos-like immunoreactivity in spinal dorsal horn regions
944 associated with nociceptive processing. PSD95–nNOS
945 inhibitors were maximally efficacious in suppressing
946 formalin-evoked Fos protein expression in the superficial
947 dorsal horn of the spinal cord. Only MK-801 reliably
948 decreased Fos expression in the ventral horn. Thus it is
949 noteworthy that although MK-801 has well-established
950 antinociceptive properties in the formalin test (Vaccarino
951 et al., 1993; Chaplan et al., 1997), the dose used in the
952 current study also produced modest motor impairment
953 in the rotarod test in our study but did not prevent rats
954 from navigating a radial arm maze used to assess spatial
955 memory performance in our previous work (Smith et al.,
956 2016).

957 An important observation of our study was that
958 PSD95–nNOS disruptors suppressed formalin-evoked
959 pain behavior and spinal neuronal activation in the same
960 animals and at doses that did not produce motor
961 impairment characteristic of the non-competitive
962 NMDAR antagonist MK-801. Neither IC87201 nor ZL006
963 produced motor impairment associated with the
964 noncompetitive NMDAR antagonist MK-801 in rat
965 subjects. ZL006 has previously been reported to not
966 impair spatial memory in mice whereas the nNOS
967 inhibitor 7-nitroindazole decreased spatial memory
968 (Zhou et al., 2010). However, lack of observable impair-
969 ments in spatial memory tasks is not sufficient to conclude
970 that memory impairment is absent following pharmaco-
971 logical manipulations. Previous work by our group showed
972 that MK-801 (at the same dose employed in the present
973 study) eliminated memory for source of origin of informa-
974 tion (i.e. source memory) under conditions in which spatial
975 memory was spared (Smith et al., 2016). By contrast,
976 ZL006 and IC87201, at the highest efficacious doses
977 evaluated in the present study, did not impair spatial or
978 source memory in rats under identical testing conditions
979 (Smith et al., 2016). Even at supramaximal doses
980 (30 mg/kg), IC87201 and ZL006 did not produce motor
981 impairment or alter basal nociceptive thresholds in mice
982 in our previous work (Lee et al., 2015). These observa-
983 tions collectively suggest that disruption of PSD95–nNOS
984 interactions may exhibit better therapeutic ratios com-
985 pared to NMDAR antagonists. PSD95–nNOS inhibitors
986 are also likely to exhibit limited side effect profiles com-
987 pared to NOS inhibitors because NOS inhibitors are not

selective for nNOS but inhibit other NOS isoforms 988
(e.g. eNOS), that similarly translates into unwanted side 989
effects (Rees et al., 1989; Kobayashi et al., 1991). Thus, 990
non-specific amino acid NOS inhibitors (Bohme et al., 991
1993; Rickard and Gibbs, 2003; Koylu et al., 2005), 992
selective indazole nNOS inhibitors (Holscher et al., 993
1996; Yildiz Akar et al., 2007) and genetic deletion of 994
nNOS (Weitzdoerfer et al., 2004) also produce impair- 995
ments in cognitive functioning, learning and memory. In 996
conclusion, the pattern of antinociceptive efficacy, 997
suppression of inflammation-evoked neuronal activation 998
in lumbar spinal dorsal horn, and lack of side effects pro- 999
duced by ZL006 and IC87201 (see also (Lee et al., 2015; 1000
Smith et al., 2016)) suggest that small molecule nNOS/ 1001
PSD95 protein–protein interaction inhibitors should 1002
exhibit a superior therapeutic index compared with 1003
NMDAR antagonists and may represent a safer, effective 1004
mechanism to alleviate chronic pain. 1005

FUNDING

This work was supported by the National Institute on Drug 1006
Abuse [DA037673 (AGH and YYL)] and the National 1007
Cancer Institute [CA200417 (AGH)]. LMC is supported 1008
by a T32 training grant DA024628 and the Harlan 1009
Scholars Research Program. 1010
1011

CONFLICT OF INTEREST

YYL is partially employed at Anagin, LLC. 1012
1013

REFERENCES

- Aley KO, McCarter G, Levine JD (1998) Nitric oxide signaling in pain 1015
and nociceptor sensitization in the rat. *J Neurosci* 18:7008–7014. 1016
- Bohme GA, Bon C, Lemaire M, Reibaud M, Piot O, Stutzmann JM, 1017
Doble A, Blanchard JC (1993) Altered synaptic plasticity and 1018
memory formation in nitric oxide synthase inhibitor-treated rats. 1019
Proc Natl Acad Sci U S A 90:9191–9194. 1020
- Carey LM, Slivicki RA, Leishman E, Cornett B, Mackie K, Bradshaw 1021
H, Hohmann AG (2016) A pro-nociceptive phenotype unmasked 1022
in mice lacking fatty-acid amide hydrolase. *Mol Pain* 12. 1023
- Chaplan SR, Malmberg AB, Yaksh TL (1997) Efficacy of spinal 1024
NMDA receptor antagonism in formalin hyperalgesia and nerve 1025
injury evoked allodynia in the rat. *J Pharmacol Exp Ther* 1026
280:829–838. 1027
- Deng L, Guindon J, Vemuri VK, Thakur GA, White FA, Makriyannis A, 1028
Hohmann AG (2012) The maintenance of cisplatin- and 1029
paclitaxel-induced mechanical and cold allodynia is suppressed 1030
by cannabinoid CB(2) receptor activation and independent of 1031
CXCR4 signaling in models of chemotherapy-induced peripheral 1032
neuropathy. *Mol Pain* 8:71. 1033
- Deng L, Lee WH, Xu Z, Makriyannis A, Hohmann AG (2016) 1034
Prophylactic treatment with the tricyclic antidepressant 1035
desipramine prevents development of paclitaxel-induced 1036
neuropathic pain through activation of endogenous analgesic 1037
systems. *Pharmacol Res* 114:75–89. 1038
- Doucet MV, Levine H, Dev KK, Harkin A (2013) Small-molecule 1039
inhibitors at the PSD-95/nNOS interface have antidepressant-like 1040
properties in mice. *Neuropsychopharmacology* 38:1575–1584. 1041
- Florio SK, Loh C, Huang SM, Iwamaye AE, Kitto KF, Fowler KW, 1042
Treiberg JA, Hayflick JS, Walker JM, Fairbanks CA, Lai Y (2009) 1043
Disruption of nNOS-PSD95 protein-protein interaction inhibits 1044
acute thermal hyperalgesia and chronic mechanical allodynia in 1045
rodents. *Br J Pharmacol* 158:494–506. 1046

- Franklin KB, Abbott FV (1993) Pentobarbital, diazepam, and ethanol abolish the interphase diminution of pain in the formalin test: evidence for pain modulation by GABAA receptors. *Pharmacol Biochem Behav* 46:661–666.
- Guindon J, Gujjarro A, Piomelli D, Hohmann AG (2011) Peripheral antinociceptive effects of inhibitors of monoacylglycerol lipase in a rat model of inflammatory pain. *Br J Pharmacol* 163:1464–1478.
- Holscher C, McGlinchey L, Anwyl R, Rowan MJ (1996) 7-Nitro indazole, a selective neuronal nitric oxide synthase inhibitor in vivo, impairs spatial learning in the rat. *Learn Mem* 2:267–278.
- Hyliden JL, Nahin RL, Traub RJ, Dubner R (1989) Expansion of receptive fields of spinal lamina I projection neurons in rats with unilateral adjuvant-induced inflammation: the contribution of dorsal horn mechanisms. *Pain* 37:229–243.
- Ji RR, Kohno T, Moore KA, Woolf CJ (2003) Central sensitization and LTP: do pain and memory share similar mechanisms? *Trends Neurosci* 26:696–705.
- Ji RR, Woolf CJ (2001) Neuronal plasticity and signal transduction in nociceptive neurons: implications for the initiation and maintenance of pathological pain. *Neurobiol Dis* 8:1–10.
- Kaneko M, Hammond DL (1997) Role of spinal gamma-aminobutyric acidA receptors in formalin-induced nociception in the rat. *J Pharmacol Exp Ther* 282:928–938.
- Kitto KF, Haley JE, Wilcox GL (1992) Involvement of nitric oxide in spinally mediated hyperalgesia in the mouse. *Neurosci Lett* 148:1–5.
- Kobayashi Y, Ikeda K, Shinozuka K, Nara Y, Yamori Y, Hattori K (1991) L-nitroarginine increases blood pressure in the rat. *Clin Exp Pharmacol Physiol* 18:397–399.
- Koylu EO, Kanit L, Taskiran D, Dagci T, Balkan B, Pogun S (2005) Effects of nitric oxide synthase inhibition on spatial discrimination learning and central DA2 and mACh receptors. *Pharmacol Biochem Behav* 81:32–40.
- Krystal JH, Karper LP, Seibyl JP, Freeman GK, Delaney R, Bremner JD, Heninger GR, Bowers Jr MB, Charney DS (1994) Subanesthetic effects of the noncompetitive NMDA antagonist, ketamine, in humans. Psychotomimetic, perceptual, cognitive, and neuroendocrine responses. *Arch Gen Psychiatry* 51:199–214.
- Latremoliere A, Woolf CJ (2009) Central sensitization: a generator of pain hypersensitivity by central neural plasticity. *J Pain* 10:895–926.
- Lebrun P, Manil J, Colin F (2000) Formalin-induced central sensitization in the rat: somatosensory evoked potential data. *Neurosci Lett* 283:113–116.
- Lee WH, Xu Z, Ashpole NM, Hudmon A, Kulkarni PM, Thakur GA, Lai YY, Hohmann AG (2015) Small molecule inhibitors of PSD95-nNOS protein-protein interactions as novel analgesics. *Neuropharmacology* 97:464–475.
- Ma QP, Woolf CJ (1995) Noxious stimuli induce an N-methyl-D-aspartate receptor-dependent hypersensitivity of the flexion withdrawal reflex to touch: implications for the treatment of mechanical allodynia. *Pain* 61:383–390.
- Meller ST, Gebhart GF (1993) Nitric oxide (NO) and nociceptive processing in the spinal cord. *Pain* 52:127–136.
- Miclescu A, Gordh T (2009) Nitric oxide and pain: 'Something old, something new'. *Acta Anaesthesiol Scand* 53:1107–1120.
- Nackley AG, Makriyannis A, Hohmann AG (2003a) Selective activation of cannabinoid CB(2) receptors suppresses spinal fos protein expression and pain behavior in a rat model of inflammation. *Neuroscience* 119:747–757.
- Nackley AG, Suplita 2nd RL, Hohmann AG (2003b) A peripheral cannabinoid mechanism suppresses spinal fos protein expression and pain behavior in a rat model of inflammation. *Neuroscience* 117:659–670.
- Pal HR, Berry N, Kumar R, Ray R (2002) Ketamine dependence. *Anaesth Intensive Care* 30:382–384.
- Paul-Clark MJ, Gilroy DW, Willis D, Willoughby DA, Tomlinson A (2001) Nitric oxide synthase inhibitors have opposite effects on acute inflammation depending on their route of administration. *J Immunol* 166:1169–1177.
- Prast H, Philippu A (2001) Nitric oxide as modulator of neuronal function. *Prog Neurobiol* 64:51–68.
- Presley RW, Menetrey D, Levine JD, Basbaum AI (1990) Systemic morphine suppresses noxious stimulus-evoked Fos protein-like immunoreactivity in the rat spinal cord. *J Neurosci* 10:323–335.
- Puig S, Sorkin LS (1996) Formalin-evoked activity in identified primary afferent fibers: systemic lidocaine suppresses phase-2 activity. *Pain* 64:345–355.
- Rahn EJ, Deng L, Thakur GA, Vemuri K, Zvonok AM, Lai YY, Makriyannis A, Hohmann AG (2014) Prophylactic cannabinoid administration blocks the development of paclitaxel-induced neuropathic nociception during analgesic treatment and following cessation of drug delivery. *Mol Pain* 10:27.
- Rahn EJ, Thakur GA, Wood JA, Zvonok AM, Makriyannis A, Hohmann AG (2011) Pharmacological characterization of AM1710, a putative cannabinoid CB2 agonist from the cannabillactone class: antinociception without central nervous system side-effects. *Pharmacol Biochem Behav* 98:493–502.
- Rahn EJ, Zvonok AM, Thakur GA, Khanolkar AD, Makriyannis A, Hohmann AG (2008) Selective activation of cannabinoid CB2 receptors suppresses neuropathic nociception induced by treatment with the chemotherapeutic agent paclitaxel in rats. *J Pharmacol Exp Ther* 327:584–591.
- Rees DD, Palmer RM, Moncada S (1989) Role of endothelium-derived nitric oxide in the regulation of blood pressure. *Proc Natl Acad Sci U S A* 86:3375–3378.
- Rickard NS, Gibbs ME (2003) Effects of nitric oxide inhibition on avoidance learning in the chick are lateralized and localized. *Neurobiol Learn Mem* 79:252–256.
- Sattler R, Xiong Z, Lu WY, Hafner M, MacDonald JF, Tymianski M (1999) Specific coupling of NMDA receptor activation to nitric oxide neurotoxicity by PSD-95 protein. *Science* 284:1845–1848.
- Shekar A, Fitz SD, Johnson PL, Hohmann AG, Widlanski T, Lai Y.Y. (2012) Post-trauma disruption of nNOS-PSD95 protein-protein interaction is an effective means to ameliorate conditioned fear. In: *Society for Neuroscience*, vol. 42 New Orleans, LA, USA.
- Smith AE, Xu Z, Lai YY, Kulkarni PM, Thakur GA, Hohmann AG, Crystal JD (2016) Source memory in rats is impaired by an NMDA receptor antagonist but not by PSD95-nNOS protein-protein interaction inhibitors. *Behav Brain Res* 305:23–29.
- South SM, Kohno T, Kaspar BK, Hegarty D, Vissel B, Drake CT, Ohata M, Jenab S, Sailer AW, Malkmus S, Masuyama T, Horner P, Bogulavsky J, Gage FH, Yaksh TL, Woolf CJ, Heinemann SF, Inturrisi CE (2003) A conditional deletion of the NR1 subunit of the NMDA receptor in adult spinal cord dorsal horn reduces NMDA currents and injury-induced pain. *J Neurosci* 23:5031–5040.
- Tao F, Tao YX, Gonzalez JA, Fang M, Mao P, Johns RA (2001) Knockdown of PSD-95/SAP90 delays the development of neuropathic pain in rats. *Neuroreport* 12:3251–3255.
- Tao YX, Huang YZ, Mei L, Johns RA (2000) Expression of PSD-95/SAP90 is critical for N-methyl-D-aspartate receptor-mediated thermal hyperalgesia in the spinal cord. *Neuroscience* 98:201–206.
- Tsou K, Lowitz KA, Hohmann AG, Martin WJ, Hathaway CB, Bereiter DA, Walker JM (1996) Suppression of noxious stimulus-evoked expression of Fos protein-like immunoreactivity in rat spinal cord by a selective cannabinoid agonist. *Neuroscience* 70:791–798.
- Vaccarino AL, Marek P, Kest B, Weber E, Keana JF, Liebeskind JC (1993) NMDA receptor antagonists, MK-801 and ACEA-1011, prevent the development of tonic pain following subcutaneous formalin. *Brain Res* 615:331–334.
- Vitecek J, Lojek A, Valacchi G, Kubala L (2012) Arginine-based inhibitors of nitric oxide synthase: therapeutic potential and challenges. *Mediators Inflamm* 2012:318087.
- Wang Z, Zhao Y, Jiang Y, Lv W, Wu L, Wang B, Lv L, Xu Q, Xin H (2015) Enhanced anti-ischemic stroke of ZL006 by T7-conjugated PEGylated liposomes drug delivery system. *Sci Rep* 5:12651.
- Weitzdoerfer R, Hoeger H, Engidawork E, Engelmann M, Singewald N, Lubec G, Lubec B (2004) Neuronal nitric oxide synthase knock-out mice show impaired cognitive performance. *Nitric oxide* 10:130–140.

- 1189 Woolf CJ, Thompson SW (1991) The induction and maintenance of
1190 central sensitization is dependent on N-methyl-D-aspartic acid
1191 receptor activation; implications for the treatment of post-injury
1192 pain hypersensitivity states. *Pain* 44:293–299.
- 1193 Wu J, Fang L, Lin Q, Willis WD (2001) Nitric oxide synthase in spinal
1194 cord central sensitization following intradermal injection of
1195 capsaicin. *Pain* 94:47–58.
- 1196 Yildiz Akar F, Ulak G, Tanyeri P, Erden F, Utkan T, Gacar N (2007) 7-
1197 Nitroindazole, a neuronal nitric oxide synthase inhibitor, impairs
passive-avoidance and elevated plus-maze memory performance
in rats. *Pharmacol Biochem Behav* 87:434–443.
- Zhou HY, Chen SR, Pan HL (2011) Targeting N-methyl-D-aspartate
receptors for treatment of neuropathic pain. *Expert Rev Clin
Pharmacol* 4:379–388.
- Zhou L, Li F, Xu HB, Luo CX, Wu HY, Zhu MM, Lu W, Ji X, Zhou QG,
Zhu DY (2010) Treatment of cerebral ischemia by disrupting
ischemia-induced interaction of nNOS with PSD-95. *Nat Med*
16:1439–1443.

1207
1208
1209

(Received 25 July 2016, Accepted 27 February 2017)
(Available online xxxx)

UNCORRECTED PROOF